Electronic Supplementary Material (ESI) for Lab on a Chip.

ELECTRONIC SUPPLEMENTARY INFORMATION (ESI)

Supplementary Movie S1

Finite Element Method (FEM) simulation of the PDMS membrane deflection in a pressure range from 0 to 2 bar. The video was generated from a sequence of COMSOL simulations.

Supplementary Movie S2

Sorting process of L2 larvae from a mixed population of L2, L3 and adults. The video was recorded by a KEYENCE VHX-700F microscope and run at real speed.

Supplementary Movie S3

Sorting process of embryos from a mixed population of embryos and adults. The video was recorded by a KEYENCE VHX-700F microscope and run at real speed.

S1. Evaluation of D_{pass} for different PDMS membrane thicknesses and mixing ratios

Finite Element Method (FEM) simulations (Comsol) of the membrane deflection have been carried out for different PDMS membrane thicknesses and mixing ratios in order to evaluate D_{pass}, as depicted in Fig. S1. The Mooney-Rivlin model for the hyperelastic properties of PDMS was used to simulate the membrane deflection (see Supplementary Movie S1). The relevant coefficients used in the Mooney-Rivlin model are shown in Table S1[1]. Computational results for the 25 μm membrane correspond well to our experimental results represented by green dots in Fig. S1a (see also Table 1 in the main article). Fig. S1a also shows the variation of D_{pass} as a function of applied pressure for thinner or thicker membranes, respectively. Furthermore, D_{pass} is also a function of the PDMS mixing ratio (base to curing agent), as is shown in Fig. S1b for three different ratios. Increasing the amount of base with respect to curing agent (from 5:1 to 15:1) lowers the elastic modulus, resulting in stronger membrane deflection for the same pressure value.

Table S1. Material constants of the Mooney-Rivlin model for different PDMS mixing ratios, as reported in ref. 1.

	PDMS (Ratio base:curing agent)		
Mooney-Rivlin model material constant	Ratio 5:1 (MPa)	Ratio 10:1 (MPa)	Ratio 15:1 (MPa)
C10	0	0.0308307	0.0013643
C01	0.1342	0	0.0878638
C11	0.0889167	0.0269727	0.0109259

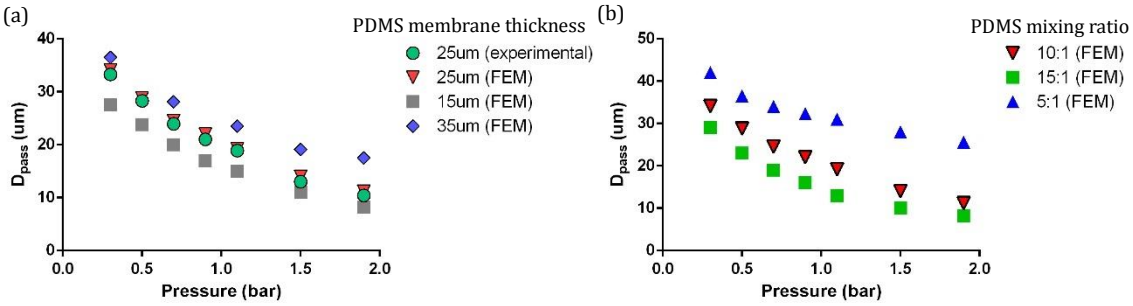

Fig. S1 Finite Element Method (FEM) simulations of the deflected PDMS membrane of a filter valve (such as V2, for instance). (a) The graph shows the influence of the PDMS membrane thickness on D_{pass} (base:curing agent ratio 10:1). For the 25 μm membrane used in our device, the simulated values agree well to the experimentally observed ones reported in Table 1. (b) Influence of the PDMS base:curing agent mixing ratio on D_{pass} (membrane thickness 25 μm).

S2. Photographs from larvae and adult worm sorting experiments

Four groups of experiments were used to evaluate the sorting accuracy of the device, as depicted in Fig. S2. The images are snapshot photographs of representative events occurring during the separation of L1 from L2 (Fig. S2a,b), L2 from L3 (Fig. S2c,d), L3 from L4 (Fig. S2e,f), and L4 from adults (Fig. S2g,h), respectively. The used protocol for these sorting experiments is similar for all stages, but pressure values, in particular the pressure applied to the valve V2, were adjusted to enable sorting of a certain worm stage/size (see Table 1).

As a representative example, L2 sorting from L3 and adult worms has been explained already in full detail in the article (see also Fig 4a-c).

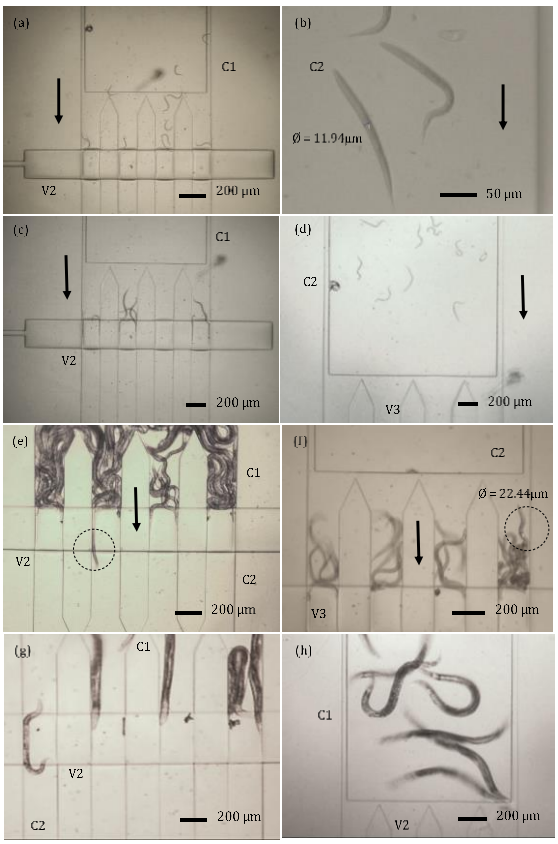

Fig. S2 Images of size-selective on-chip sorting of L1 from L2 (a,b), L2 from L3 (c,d), L3 from L4 (e,f), and L4 from adults (g,h). (a) Before sorting, heterogeneous populations comprising L1 and L2 larvae were loaded into chamber C1 (V2 closed). (b) Photograph of L1 larvae in chamber C2 after successful L1 sorting; only L1 larvae are in C2. In order to determine safely the larval stage, the diameter of all larvae present in C2 was measured with a microscope (KEYENCE VHX-700F) and compared with typical values listed in Table 1 of the main article. We measured a mean maximum diameter of 11.9±0.2 µm corresponding to the L1 larval stage indeed. (c) Snapshot of L2 larvae passing through valve V2, to which a pressure P2 has been applied. L3 larvae are blocked by V2. (d) Photograph of chamber C2 containing only L2 larvae after sorting from a L2&L3 population in chamber C1. (e) Snapshot of a L3 larva passing through the valve V2 (indicated by the dashed circle), to which a pressure P3 has been applied. L4 larvae are seen to be retained in C1 by valve V2. (f) After transfer of L3 larvae from C1 to C2, L3 larvae were blocked in chamber C2 by valve V3 for counting and imaging. The measured average diameter of the L3 larvae was 22.4±0.2 µm. (g) Snapshot of a L4 larva passing through valve V2, to which a pressure P4 has been applied. (h) Successful adult sorting from a mixed L4&adult population, as evidenced by the presence of only adults in C1 after selective transfer of L4 to C2.

S3. Detailed analysis of throughput of the sorting experiments

Sorting throughput in our device appeared to be a function of target worm density in chamber C1. We evaluated this relationship by counting the number of target worms passing through the filter structure during subsequent time windows (of 10 s duration) in the course of a sorting experiment. Density of target worms was defined as the actual average target worm number in C1 for each time window divided by the chamber volume of 1.2 µL. According to our experiments, throughput for "larva & larva" separation is comparable for all protocols, *i.e.* separation of L1 from L2, L2 from L3, and L3 from L4, whereas the separation speed of L4 from adults showed a slightly different behavior. Thus, two groups of the experiments, larva & larva populations and a L4 & adult population, were used to evaluate the throughput. For all experiments we observe a decreasing sorting speed (throughput) as the sorting process progresses and the target worm density in C1 is decreases. Data comparing L2&L3 and L4 & adult sorting experiments are shown in Fig. S3. In particular, in the beginning of the sorting experiment, we determined a throughput of approximately 3.5 worms/sec (210 worms/min) for the larva & larva populations and around 3.0 worms/s (180 worms/min) for the L4 & adult population for a target worm density in the range of 30 to 40 worms/µL. The slightly lower value in the latter case may be due to the fact larger size L4 larvae require a longer transfer time through the filter structure compared to smaller larvae. Towards the end of an experiment, when the number of target worms in C1 strongly decreases, throughput approaches a value of about 0.3-0.5 worms/sec (20-30 worms/min) for larva & larva sorting, whereas for L4 & adult sorting throughput remains slightly higher, i.e. about 1.0-1.5 worms/sec (60-90 worms/min). A possible reason for this observation is that adult worm-related hindrance at the height step at the chamber/valve interface (see Fig. 1a) has stronger impact at lower worm densities. During larva & larva separation, even at low densities, some of the larger larvae can still temporally block the valve channel, thus reducing slightly the throughput, whereas in L4 & adult separation, adults cannot approach the valve structure (see Fig. 4a and Supplementary Movie S2).

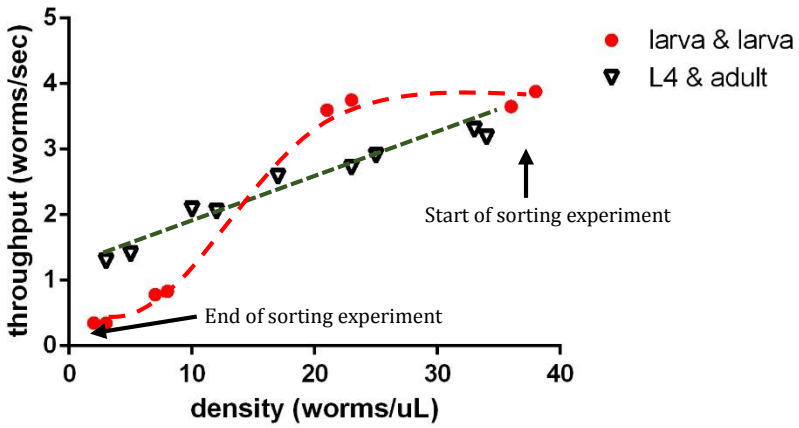

Fig. S3 Time-dependent throughput during the lapse of a sorting experiment, in particular for L2&L3 and L4 & adult sorting experiments (2 experiments for each case). The initial worm density is about 40 worms/µL, which decreases to 0 worms/µL at the end of the sorting process. Data was analyzed at different stages of the sorting progress, *i.e.* for decreasing target worm densities in chamber C1. The dashed lines are only intended to be a guide to the eye.

References

1 Tae Kyung Kim, Jeong Koo Kim, Ok Chan Jeong, Measurement of nonlinear mechanical properties of PDMS elastomer, Microelectronic Engineering, Volume 88, Issue 8, August 2011, Pages 1982-1985, ISSN 0167-9317